# Dorsal Motor Vagal Neurons Can Elicit Bradycardia and Reduce Anxiety-Like Behavior

Misty M. Strain[1]*, Nicholas J. Conley[2]*, Lily S. Kauffman[2]*, Liliana Espinoza[1], Stephanie Fedorchak[1], Patricia Castro Martinez[3], Maisie E. Crook[2], Maira Jalil[2], Georgia E. Hodes[4], Stephen B. G. Abbott[5], Ali D. Güler[2], John N. Campbell[2#] and Carie R. Boychuk[1,6#]

**co-first authors*
*[#] co-corresponding authors*

[1] Department of Cellular and Integrative Physiology, Long School of Medicine, University of Texas Health San Antonio, San Antonio, TX
[2] Department of Biology, University of Virginia, Charlottesville, VA
[3] Neuroscience Undergraduate Major, University of Virginia, Charlottesville, VA
[4] School of Neuroscience, Virginia Polytechnic Institute and State University, Blacksburg, VA
[5] Department of Pharmacology, University of Virginia, Charlottesville, VA
[6] Dalton Cardiovascular Research Center, University of Missouri, Columbia, MO

Running Title: Activating DMV reduces HR and anxiety.

Correspondence to:
Carie R. Boychuk, Ph.D. (lead contact)
Dalton Cardiovascular Research Center
Department of Biomedical Sciences
University of Missouri
College of Veterinary Medicine
1500 Research Park Drive
Columbia, Missouri 65203, USA
Telephone: 210-450-8449
Fax: 210-567-4410
Email: boychukc@missouri.edu

John N. Campbell, Ph.D.
Department of Biology
University of Virginia
485 McCormick Road
PO BOX 400328
Charlottesville, VA 22903, USA
Email: jnc4e@virginia.edu

Keywords: autonomic regulation, parasympathetic nervous system
Number of pages: 47
Number of figures: 4
Number of words in Abstract: 142

Number of words in Body: 5316
Total words: 12577
References: 75

**SUMMARY:**

Cardiovagal neurons (CVNs) innervate cardiac ganglia through the vagus nerve to control cardiac function. Although the cardioinhibitory role of CVNs in nucleus ambiguus ($CVN^{NA}$) is well established, the nature and functionality of CVNs in dorsal motor nucleus of the vagus ($CVN^{DMV}$) is less clear. We therefore aimed to characterize $CVN^{DMV}$ anatomically, physiologically, and functionally. Optogenetically activating cholinergic DMV neurons resulted in robust bradycardia through peripheral muscarinic (parasympathetic) and nicotinic (ganglionic) acetylcholine receptors, but not beta-1-adrenergic (sympathetic) receptors. Retrograde tracing from the cardiac fat pad labeled $CVN^{NA}$ and $CVN^{DMV}$ through the vagus nerve. Using whole cell patch clamp, $CVN^{DMV}$ demonstrated greater hyperexcitability and spontaneous action potential firing *ex vivo* despite similar resting membrane potentials, compared to $CVN^{NA}$. Chemogenetically activating DMV also caused significant bradycardia with a correlated reduction in anxiety-like behavior. Thus, DMV contains uniquely hyperexcitable CVNs capable of cardioinhibition and robust anxiolysis.

69 **INTRODUCTION:**

70 Cardiovagal neurons (CVNs) send axonal projections from hindbrain to cardiac
71 ganglia through the vagus nerve to elicit cardioinhibitory (i.e., slowing of heart rate; HR)
72 action at rest and during critical cardiorespiratory homeostatic reflexes. Although in
73 mammals most CVNs are found in the nucleus ambiguus ($CVN^{NA}$), 20% of CVNs arise
74 from a second region, the dorsal motor nucleus of the vagus ($CVN^{DMV}$) [1-6]. While the ability
75 of $CVN^{NA}$ to control chronotropy (e.g. HR) is well characterized [7-9], whether this ability
76 extends to $CVN^{DMV}$ remains controversial, despite their extensive innervation of cardiac
77 tissue [10]. $CVN^{DMV}$ innervate cardiac tissue with unmyelinated, C fibers [11], the selective
78 activation of which causes a bradycardia (or a decrease in HR) in multiple mammalian
79 species [12,13]. In addition, studies of CVN ontogenesis implicate DMV, not NA, as the
80 primary vagal nucleus in lower-order vertebrates and in early mammalian embryonic
81 development, since $CVN^{NA}$ migrate out of DMV [14,15], making it possible that $CVN^{DMV}$ retain
82 functional cardioinhibitory activity in mammals.

83 Despite these anatomical studies, functional studies remain conflicting. Some
84 argue that direct electrical stimulation of DMV does not change chronotropy [7,16], while
85 others demonstrate local activation (chemical, electrical, optogenetic, or chemogenetic)
86 elicits bradycardias even if only modestly [17-21]. However, no activation technique in awake
87 animals used to date rules out incidental stimulation of either neighboring nucleus tractus
88 solitarius (NTS) neurons or inhibitory interneurons within DMV. Stimulation of this latter
89 population could significantly dampen the impact of cholinergic premotor neuron
90 stimulation. Thus, whether cholinergic $CVN^{DMV}$ are capable of controlling chronotropy
91 remains an important but open question.

92 A recent resurgence of interest in understanding of vagal physiology is driven by
93 the growing number of therapeutic applications for vagus nerve stimulation [22]. Of
94 particular interest, vagus nerve stimulation is a promising treatment for anxiety and post-
95 traumatic stress disorder [23,24]. In rats, stimulating the vagus nerve accelerates extinction
96 of conditioned fear [25,26] and decreases anxiety-like behavior in the elevated plus maze
97 paradigm [23]. In humans, vagal nerve stimulation may even reduce treatment-resistant
98 anxiety disorders [27]. However, the mechanism behind the anxiolytic effect of vagal
99 stimulation is currently unknown. Since the vagus nerve is a bidirectional nerve, carrying
100 sensory information from viscera to brain and motor information from brain to viscera, the
101 extent to which the anxiolytic effect of vagus nerve stimulation depends on sensory or
102 motor signaling is unclear. One possibility is that activating the vagus nerve decreases
103 anxiety by slowing HR, in line with the James-Lange theory of emotions [28]. Accordingly,
104 a recent study in mice demonstrated that tachycardia (e.g. increase in HR) is sufficient to
105 induce anxiety-like behavior [29].

106 Controversy over the role of $CVN^{DMV}$ may stem in part from differences in $CVN^{NA}$
107 and $CVN^{DMV}$ electrophysiology and thus their roles in regulating HR. Notably, $CVN^{NA}$ are
108 largely quiescent *in vivo* and *ex vivo* [30,31], responding solely to integrated synaptic
109 signaling. While limited data exist on the electrophysiological properties of $CVN^{DMV}$
110 specifically, other DMV neuronal populations have unique pace-making properties and
111 maintain a relatively high activity *ex vivo* [32], which allows for more complex signal
112 processing. One investigation into their activity also suggests that, unlike $CVN^{NA}$, $CVN^{DMV}$
113 do not demonstrate robust respiratory burst patterning [33]. Therefore, it is tempting to
114 speculate that $CVN^{DMV}$ integrate and communicate central information differently from

115 $CVN^{NA}$ and represent a functionally unique circuit with respect to $CVN^{NA}$, which is
116 consistent with evidence that $CVN^{DMV}$ and $CVN^{NA}$ target different cardiac ganglia [34]. A
117 more extensive characterization of the electrophysiological properties of $CVN^{DMV}$ will help
118 build a foundation for understanding their cardioregulatory role, and importantly, for
119 harnessing the therapeutic potential of vagus nerve stimulation. This is critical given that
120 synaptic input to $CVN^{DMV}$ is uniquely sensitive to perturbation of the cardiovascular
121 system, relative to $CVN^{NA}$ [35].

122 The aim of the present study was to characterize the ability of DMV neurons to
123 regulate HR functionally, physiologically, and pharmacologically. We hypothesized that
124 activating choline acetyltransferase positive (Chat+) $CVN^{DMV}$ elicits robust bradycardias.
125 Moreover, we sought to characterize the electrophysiological properties of $CVN^{DMV}$ to
126 determine whether they are distinct from the more extensively studied $CVN^{NA}$. Testing of
127 these hypotheses was accomplished using a combination of opto- and chemogenetic
128 stimulation specifically in Chat+ neurons, pharmacology techniques to determine the
129 regulatory role of $CVN^{DMV}$ on chronotropy, and retrograde labeling paired with
130 electrophysiology procedures to examine differences between the two CVN populations.
131 Our results raise the possibility that $CVN^{DMV}$ play a role distinct from $CVN^{NA}$ in regulating
132 HR.

133

134 **RESULTS**

135 **Optogenetic stimulation of Chat+ DMV can elicit bradycardia:** To determine if
136 $CVN^{DMV}$ activation is capable of cardioinhibition, we used optogenetics to activate
137 cholinergic neurons in DMV. Specifically, we crossed Ai32 mice expressing

138 channelrhodopsin-2/EYFP fusion protein (ChR2) to loxP floxed choline acetyltransferase
139 (Chat$^{cre}$) mice to selectively express ChR2 in Chat+ neurons (Chat$^{cre}$;ChR2).
140 Chat$^{cre}$;ChR2 and Chat$^{cre}$ mice (Figure 1A) were implanted with HR telemetry devices and
141 fiber optic probes above the right DMV. HR was examined before and during
142 photostimulation. A preliminary study found that 20 Hz (-261 ± 32 bpm; n = 4 mice) elicited
143 a significantly larger bradycardia compared to 5 (-58 ± 28 bpm; repeated measure one-
144 way ANOVA with Šídák's post-hoc, $p$ = 0.0003), 10 (-126 ± 26 bpm; $p$ = 0.0064), and 40
145 (-43 ± 16 bpm; $p$ = 0.0002) Hz stimulation to DMV in Chat$^{cre}$;ChR2 mice (data not shown).
146 We further verified that DMV neurons were continuously activated by 20 Hz
147 photostimulation using whole-cell patch-clamp in brain slices from Chat$^{cre}$;ChR2 mice
148 (before: 2.5 ± 1.4 Hz versus during: 13.0 ± 2.7 Hz; repeated measure one-way ANOVA
149 with Tukey's post-hoc, $p$ = 0.0482; n = 5 neurons from two mice; Figure 1B). DMV neurons
150 from Chat$^{cre}$;ChR2 mice also had lower firing frequencies immediately following
151 stimulation (after: 1.4 ± 1.2 Hz; $p$ = 0.0321), and they qualitatively demonstrated a pause
152 immediately following stimulation termination that lasted for 10.3 ± 3.9 s with a range of
153 0.7 to 18 s.

154 Photostimulating DMV in awake male and female Chat$^{cre}$;ChR2 mice significantly
155 affected HR compared to Chat$^{cre}$ mice. During photostimulation, Chat$^{cre}$;ChR2 decreased
156 HR (271 ± 17 bpm) compared to HR before stimulation (605 ± 18 bpm; repeated measure
157 two-way ANOVA with Šídák's post-hoc, $p$ < 0.0001; n = 13 mice; Figure 1F, G).
158 Photostimulation failed to significantly affect HR during stimulation in control, Chat$^{cre}$ mice
159 (before: 597 ± 61 bpm vs. during: 606 ± 31 bpm, $p$ = 0.9633; n = 4 mice), confirming that
160 photostimulation-induced bradycardia in Chat$^{cre}$;ChR2 was not a consequence of off-

161 target effects or exposure to a laser (e.g., tissue necrosis, light diffusion, temperature
162 effects). Finally, photostimulation-induced bradycardia in Chat$^{cre}$;ChR2 was significantly
163 different from HR responses to light in Chat$^{cre}$ control (comparing both mouse lines during
164 stimulation: $p < 0.0001$).

165 In contrast to photoexcitation of DMV neurons, photoinhibition of cholinergic
166 neurons in DMV of awake mice using Chat$^{cre}$ mice crossed to Ai39 mice conditionally
167 expressing halorhodopsin (NpHR$^{EYFP}$), produced no significant HR response to light
168 (before: 629 ± 45 bpm vs. during: 627 ± 38 bpm; two-tailed paired Student's t-test, $p$ =
169 0.8950, n = 3 mice). While these results suggest that under these conditions DMV
170 neurons are sufficient to regulate HR but not necessary for control of resting HR, the
171 decay kinetics of NpHR$^{EYFP}$ expressed by Ai39 mice are sufficiently fast enough that it
172 might not cause a robust neural inhibition [36].

173 Since the axons of CVN$^{NA}$ travel dorsally to converge with axons from CVN$^{DMV}$
174 before turning and exiting the brainstem (e.g., [37]), it was possible that cardioinhibitory
175 actions of DMV resulted from stimulating nearby CVN$^{NA}$ axons. To rule out CVN$^{NA}$ axonal
176 stimulation, we first examined c-Fos expression in ChAT+ neurons two hours post-DMV
177 stimulation (Figure 1D). Qualitatively robust c-Fos was seen on the stimulated (right) side
178 of DMV with no c-Fos expression in NA. We also confirmed using immunofluorescence
179 that stimulating NA directly causes c-Fos expression (Figure 1J). Finally in a subset of
180 anesthetized Chat$^{cre}$;ChR2 mice, photostimulation of the exposed vagus nerve produced
181 no change in HR (before: 422 ± 61 bpm vs. during: 419 ± 60 bmp; two-tailed paired
182 Student's t-test, $p$ = 0.9723; n = 3 mice). Taken together, axonal expression of ChR2 in
183 NA was not sufficient to activate NA and elicit bradycardia.

184 **DMV photostimulation-induced bradycardia works through canonical vagal**
185 **circuits:** To confirm that DMV photostimulation affects HR though autonomic pathways,
186 male Chat$^{cre}$;ChR2 mice were administered an intraperitoneal (*i.p.)* injection of
187 hexamethonium to block all nicotinic acetylcholine receptor (nAChR) communication
188 between preganglionic and cardiac-projecting postganglionic parasympathetic neurons
189 prior to DMV (n = 4) or NA (n = 3) photostimulation (Figure 1E). Photostimulation of DMV
190 (-261 ± 32 bpm) produced as similar of a robust bradycardia as photostimulation of NA (-
191 255 ± 32 bpm) (repeated measure two-way ANOVA*,* $p$ = 0.8157). As expected,
192 pretreatment of hexamethonium abolished photostimulation-induced bradycardias
193 regardless of regions (HR responses in DMV: 3 ± 3 bpm and HR responses in NA: -2 ±
194 1, $p < 0.0001$; Figure 1J-L*)*, and HR was also not different between DMV and NA during
195 photostimulation after pre-treatment with hexamethonium (p = 0.9931).
196 To confirm that DMV photostimulation affects HR though muscarinic acetylcholine
197 receptor (mAChR) activation from postganglionic parasympathetic neurons to cardiac
198 tissue, consistent with canonical cardiovagal signaling, Chat$^{cre}$;ChR2 mice received *i.p*.
199 injections of scopolamine methylbromide (to block parasympathetic activity) and atenolol
200 (to block sympathetic activity) in a randomized order prior to photostimulation (Figure 1E).
201 In this subset of mice (n = 5), optogenetic activation of DMV neurons again induced robust
202 bradycardia (-405 ± 46 bpm) (Figure 1H, I). Although administration of atenolol modestly
203 reduced DMV light-induced bradycardias (-276 ± 39 bpm; repeated measure one-way
204 ANOVA with Tukey's post-hoc, $p$ = 0.003; Figure 1H, I), atenolol also significantly
205 decreased resting HR (before: 665 ± 21 vs. atenolol: 527 ± 10, $p$ = 0.0093; n = 5). Using
206 a simple linear regression, there was a significant negative relationship between resting

207 HR and DMV light-induced bradycardia ($R^2$ = 0.4741, $p$ = 0.0277). Therefore, it is likely
208 that the impact of atenolol on DMV-related bradycardia is through overall reductions in
209 resting HR, and not stimulation of postganglionic sympathetic pathways. Unlike atenolol,
210 however, administering scopolamine methylbromide abolished DMV light-induced
211 bradycardias (14 ± 3 bpm, $p$ = 0.002, Figure 1H. I). Thus, both nAChR and mAChR activity
212 is required for photostimulation-induced decreases in HR from DMV similar to NA. Some
213 reports suggest that DMV-mediated vagal activity on cardiac tissue occurs through non-
214 canonical nAChR communication between postganglionic parasympathetic neurons to
215 cardiac tissue [38]. However, since mAChR antagonism abolished DMV light-induced
216 bradycardias, this confirms that DMV neurons induce robust bradycardia through the
217 canonical cardiovagal pathway nAChR→mAChR signaling (and not nAChR→nAChR).

218 **DMV innervates cardiac tissue through the vagus nerve**: Retrograde tracing
219 with rhodamine and cholera toxin subunit B (CT-B) was done in male C57BL6/J mice to
220 calculate the number of $CVN^{DMV}$ and $CVN^{NA}$ labeled by each tracer (n=6-8 mice per tracer
221 for each CVN group; Figure 2A, B). Although both tracers identified positive neurons in
222 NA and DMV, there were fewer traced neurons in $CVN^{DMV}$ (31 ± 19 neurons) compared
223 to $CVN^{NA}$ regardless of tracer (99 ± 16 neurons; repeated measure two-way ANOVA with
224 Šídák's post-hoc, $p$ < 0.0001; Figure 2C). In all animals, both right and left DMV
225 contained positive labeling. In one animal examined for right versus left distribution, the
226 right DMV contained more retrograde labeling (68 neurons) compared to the left DMV (45
227 neurons). This pattern was similar to previous reports in rats [39]. In addition, CT-B (47 ±
228 36 neurons) labeled significantly fewer neurons than rhodamine regardless of region (83
229 ± 33 neurons; $p$ = 0.0472). There was not a significant interaction between CVN location

230 and tracer ($p$ = 0.8294). To confirm that retrograde labeling of $CVN^{DMV}$ required an intact
231 vagus nerve, a unilateral left vagotomy prior to cardiac injection of rhodamine was
232 performed in a separate group of animals (n = 3 mice, Figure 2D). Unilateral vagotomy
233 eliminated labeling of $CVN^{DMV}$ ipsilateral to vagotomy (2 ± 1 labeled $CVN^{DMV}$) compared
234 to the contralateral side (32 ± 8 labeled $CVN^{DMV}$; two-tailed paired Student's t-test, $p$ =
235 0.0483; Figure 2E). Taken together, DMV contains neurons that retrogradely label from
236 cardiac tissue in a vagus-dependent manner.

237 **$CVN^{DMV}$ show spontaneous firing and have larger input resistance *ex vivo***
238 **compared to $CVN^{NA}$:** To characterize the electrophysiological properties of $CVN^{DMV}$ in
239 relation to $CVN^{NA}$, additional studies examined the general excitability of CVNs in male
240 C57BL6/J mice using whole-cell patch-clamp electrophysiology under current clamp
241 configuration. Retrogradely labeled CVNs were identified using visual inspection for
242 rhodamine and anatomical landmarks (Figure 3A). Post-hoc biocytin recovery confirmed
243 location and cholinergic phenotype (Figure 3B). $CVN^{DMV}$ exhibited more spontaneous
244 firing (8/14 neurons from 10 mice) compared to $CVN^{NA}$ (0/10 neurons from 9 mice; Mann
245 Whitney test, $p$ = 0.0064), which were completely devoid of any spontaneous firing activity
246 (Figure 3C-D). Of $CVN^{DMV}$ exhibiting spontaneous firing (57%), the average frequency
247 was 1.28 ± 0.31 Hz.

248 No statistical differences in resting membrane potential were found between
249 $CVN^{DMV}$ (-58.60 ± 2.72 mV; n = 14 neurons from 10 mice) and $CVN^{NA}$ (-62.18 ± 1.75 mV;
250 n = 10 neurons from 9 mice; two-tailed unpaired Student's t-test, $p$ = 0.3256, Figure 3E).
251 However, we found that $CVN^{DMV}$ (492.00 ± 22.02 MΩ; n = 14 neurons from 10 mice)
252 demonstrated significantly larger input resistance ($R_{input}$) than $CVN^{NA}$ (158.20 ± 10.61 MΩ;

253 n = 10 neurons from 9 mice; two-tailed unpaired Student's t-test, $p < 0.0001$; Figure 3F-
254 H). Additionally, $CVN^{DMV}$ (30.0 ± 1.5 pF) were significantly smaller in size than $CVN^{NA}$
255 (61.1 ± 6.6 pF; two-tailed unpaired Student's t-test, $p<0.0001$) based on their recorded
256 capacitance.

257 **$CVN^{DMV}$ are hyperexcitable compared to $CVN^{NA}$ *ex vivo*:** To determine if there
258 were any differences in excitability between $CVN^{DMV}$ and $CVN^{NA}$, CVNs were examined
259 for general excitability through stepped depolarizations of current (Figure 3I). As
260 expected, regardless of neuronal type, stepped current injections evoked a current
261 dependent increase in action potential frequency (repeated measure two-way ANOVA
262 with Šídák's post-hoc, $p <0.0001$; Figure 3J). Additionally, a significant effect of neuronal
263 type regardless of current injection was found, with $CVN^{DMV}$ exhibiting a significantly
264 greater number of evoked action potentials (5 ± 1 number of action potentials, n = 14
265 neurons from 10 mice) compared to $CVN^{NA}$ (2 ± 1 number of action potentials, n = 10
266 neurons from 9 mice; $p < 0.0001$). Finally, we found a significant interaction between
267 current injection and neuronal type ($p < 0.0001$), with significantly more evoked action
268 potentials in $CVN^{DMV}$ compared to the $CVN^{NA}$ at 100 (0.30 vs. 3.42 ± 0.5; $p = 0.0001$),
269 150 (0.80 vs. 5.00 ± 0.5; $p < 0.0001$), 200 (2.10 vs. 5.93 ± 0.5; $p < 0.0001$), and 250 pA
270 (3.80 vs. 6.43 ± 0.6; $p = 0.0017$); Figure 3J). Taken together, $CVN^{DMV}$ are more excitable
271 than $CVN^{NA}$.

272 **Chemogenetic activation of DMV suppresses HR for up to 8 hours:** Although
273 our optogenetic studies could rule out interneuron activity, they could not exclude the
274 possibility that off target stimulation of nearby Chat+ neurons (e.g., hypoglossal neurons)
275 affected HR. Therefore, to further confirm that activating DMV neurons specifically

276 decreases HR, we used an alternative strategy, chemogenetically activating DMV
277 neurons with the excitatory designer receptor, hM3Dq. Here, hM3Dq was specifically
278 targeted to DMV neurons through an intersectional genetics approach which leverages
279 the co-expression of *Chat* and *Phox2b* genes by DMV neurons but not by neighboring
280 neurons (i.e., hypoglossal) [40,41]. First, to validate this intersectional approach,
281 $Chat^{Cre}$;$Phox2b^{Flp}$ mice were crossed with $R26^{ds\text{-}HTB}$ mice, a reporter line which expresses
282 nuclear-localized, green fluorescent protein (GFP)-tagged histone 2b protein (H2b-GFP)
283 upon recombination by both Cre and Flp. In the resulting $Chat^{Cre}$;$Phox2b^{Flp}$;$R26^{ds\text{-}HTB}$
284 mice, essentially all peripherally-projecting DMV neurons, as labeled by a systemic (*i.p.*)
285 retrograde tracer, Fluorogold, were H2b-GFP immunofluorescent (136/139 DMV neurons
286 from four mice (97.8%) were both Fluorogold+ and H2b-GFP+; representative image in
287 Supplemental Figure 1A). These results confirm that $Chat^{Cre}$ and $Phox2b^{Flp}$ are co-
288 expressed by all DMV vagal efferent neurons and thus validate our intersectional
289 approach.

290 Next, to express hM3Dq specifically in DMV neurons, an adeno-associated virus
291 (AAV) in which Cre- and Flp- dependently expresses a hemagglutinin (HA)-tagged
292 hM3Dq (AAV1-CreON/FlpON-hM3Dq-HA; Figure 4A) was injected into DMV of male and
293 female $Chat^{Cre}$;$Phox2b^{Flp}$;$R26^{ds\text{-}HTB}$ mice. This resulted in hM3Dq-HA expression in the
294 vast majority of H2b-GFP+ DMV neurons ("DMV-hM3Dq" mice; Figures 4A-C).
295 Importantly, we failed to detect any hM3Dq-HA expression in NA (Figure 4B-C) or DMV
296 of mice lacking Cre and Flp recombinases (Supplemental Figure 1B), confirming the
297 specificity of our injection strategy and AAV expression.

298 To determine whether chemogenetically activating DMV neurons affects HR,
299 hM3Dq ligand clozapine N-oxide (CNO; 1 mg/kg; *i.p.*) was administered while measuring
300 HR by non-invasive electrocardiography (ECG; n=8 mice per genotype). Administering
301 CNO to DMV-hM3Dq mice significantly decreased HR for up to 8 hours compared to
302 baseline (baseline: 718 ± 10 bpm; 20 min: 497 ± 34 bpm, $p$ = 0.0012; 40 min: 497 ± 30
303 bpm, $p$ = 0.0008; 60 min: 467 ± 36 bpm, $p$ = 0.0007; 2hr: 469 ± 39 bpm, $p$ = 0.0011; 6hr:
304 598 ± 19 bpm, $p$ = 0.0006; 8hr: 637 ± 24 bpm, $p$ = 0.0274; Figure 4D). HR returned to
305 baseline by 24 hours post-CNO (24hr: 731 ± 9 bpm, $p$ = 0.7247). As expected, the acute
306 bradycardia after CNO administration required peripheral muscarinic signaling, as it was
307 abolished by administering the peripheral muscarinic blocker, methyl-atropine bromide
308 (MA; 1.0 mg/kg; *i.p.*), 20min after CNO (baseline: 747 ± 5 bpm; after CNO: 640 ± 19 bpm
309 *vs*. baseline, $p$ = 0.0078; after MA: 801 ± 4 bpm *vs*. baseline, $p$ = 0.0004; Figure 4E). On
310 the other hand, administering CNO to hM3Dq-negative control mice failed to significantly
311 alter HR ($p > 0.05$ *vs*. baseline or vehicle; Figure 4E; Supplemental Figure 1C), indicating
312 that CNO alone did not affect HR. These results, together with our optogenetics studies,
313 provide robust evidence that DMV neurons can decrease HR through peripheral
314 muscarinic signaling.

315 **Activating DMV neurons reduces anxiety-like behavior:** Tachycardia increases
316 anxiety-like behavior in mice [29], consistent with the James-Lange theory that physiological
317 cues can drive emotional states [28]. We therefore wondered whether the CNO-induced
318 bradycardia in DMV-hM3Dq mice corresponded to any change in anxiety-like behavior.
319 To investigate, male and female DMV-hM3Dq mice and control mice (n=8 per group)
320 were administered CNO or saline vehicle and then assessed behaviorally by the open

321 field test, an assay which measures anxiety-like behavior based on time spent in the
322 center of an open arena (Figure 4F) [42,43]. Strikingly compared to vehicle, CNO treatment
323 in DMV-hM3Dq mice significantly increased their time spent in the center of the open field
324 (CNO: 85.31 ± 17.38 s vs. Vehicle: 64.55 ± 13.98 s; two tailed paired Student's t-test, $p$
325 = 0.0379, Figure 4G). The increased time spent in the center was not due to an increase
326 in overall motility since total time spent moving did not differ significantly between saline
327 and CNO treatments (two tailed paired Student's t-test, $p$ = 0.4643, Figure 4H). In
328 addition, CNO's effects on HR and center time in DMV-hM3Dq mice were moderately
329 correlated ($R^2$ = 0.7734, $p$ = 0.0414; Figure 4I). Thus, activating DMV neurons caused a
330 correlated decrease in HR and anxiety-like behavior in the open field test.

331 To confirm the change in anxiety-like behavior, we assessed another cohort of
332 DMV-hM3Dq mice in a different measure of anxiety, the elevated plus maze [44]. CNO
333 treatment significantly increased the time DMV-hM3Dq mice spent in the open-arms of
334 an elevated plus maze, relative to vehicle treatment, indicating a decrease in anxiety-like
335 behavior (CNO: 16.9 ± 4.83 s vs. Vehicle: 0.23 ± 0.23 s, repeated measure ANOVA with
336 Tukey's post-hoc, $p$ = 0.0235; Figure 4K). CNO treatment also significantly increased
337 other signs of anxiolysis in DMV-hM3Dq mice: time spent moving (CNO: 162.6 ± 14.4 s
338 vs. Saline: 40.7 ± 8.7 s; $p$ = 0.0006; Figure 4L); head dip events (CNO: 4.149 ± 1.022
339 dips vs. Saline: 0.2414 ± 0.1424 dips; $p$ = 0.0259; Supplemental Figure 1E); and average
340 velocity (CNO: 2.339 ± 0.3068 cm/s vs. Saline, 0.6606 ± 0.2317 s, $p$ = 0.0011;
341 Supplemental Figure 1F). Importantly, however, treating hM3Dq-negative control mice
342 with CNO did not affect their open-arm time, indicating that CNO itself does not decrease
343 anxiety-like behavior ($p$ = 0.3868; Supplemental Figure 1D). In addition, co-administering

344 MA ("CNO+MA") to DMV-hM3Dq mice largely prevented CNO's effects on measures of
345 anxiolysis, indicating that anxiolysis, as with HR, require peripheral mAChR signaling
346 (Figure 4K; Supplemental Figure 1E, F). Specifically, compared to vehicle treatment,
347 CNO+MA failed to significantly affect open-arm time, time spent moving, velocity or head
348 dip events, relative to treatment with a saline vehicle ($p < 0.05$; Figure 4K, L,
349 Supplemental Figure 1D,E). As with our open field test, the decrease in HR was trended
350 towards a moderate correlation with the increase in open-arm time ($R^2 = 0.6394$, $p =$
351 $0.0878$; Figure 4M). Thus, our results show that activating DMV neurons similarly
352 decreases HR and anxiety-like behavior, and that these effects each depend on
353 peripheral muscarinic signaling.

354 To identify the muscarinic receptors mediating anxiolysis, we repeated our HR
355 and elevated plus maze studies on DMV-hM3Dq mice but used a selective inhibitor of
356 muscarinic type 2 receptors (M2), AQ-RA 741 ("AQ") [45], which does not appear to cross
357 the blood-brain barrier [46]. Administering AQ after CNO reversed the CNO-induced
358 bradycardia (repeated measure ANOVA with Tukey's post-hoc, $p = 0.0016$; Supplemental
359 Figure 1G). Importantly, in contrast to CNO alone, administering CNO with AQ (CNO+AQ)
360 did not significantly affect time spent in the open-arms relative to saline treatment ($p =$
361 $0.2560$; Figure 4N). These results suggest that activating DMV neurons decreases
362 anxiety-like behavior through a M2-dependent mechanism.

363

364 **DISCUSSION**

365 The present study characterized $CVN^{DMV}$ anatomically, physiologically, and
366 functionally. Retrograde tracing from the cardiac fat pad confirmed the presence of CVN

367 in DMV using two different tracers, rhodamine and CT-B, and this labeling required an
368 intact vagus nerve. Electrophysiological comparison of retrogradely-labeled $CVN^{DMV}$ and
369 $CVN^{NA}$ indicate distinct circuits, with $CVN^{DMV}$ being significantly more excitable with
370 higher input resistances and spontaneous activity *ex vivo* whereas $CVN^{NA}$ were not.
371 Optogenetically activating DMV neurons caused bradycardia, which was completely
372 abolished by muscarinic and nicotinic antagonism. Finally, intersectional chemogenetic
373 activation of DMV neurons also caused bradycardia and a correlated decrease in anxiety-
374 like behavior, both of which also required peripheral muscarinic signaling, as they were
375 blocked by muscarinic antagonism.

376 Previous efforts to characterize *in vivo* electrophysiological properties of DMV
377 neurons are limited, possibly a result of their prominent C-fiber phenotypes and long
378 latency conduction times [33] making typical antidromic spike identification challenging. Our
379 retrograde labeling findings are in accordance with previous reports, which suggest that
380 only ~20% of CVN exist within DMV in totality (both sides), making the likelihood of
381 recording from these numbers *in vivo* relatively low [14]. Importantly, CVNs signal
382 organization is an established example of divergent amplification, meaning that changes
383 in HR arise from modulation (activation or inhibition) of a relatively small number of CVNs
384 [30]. Therefore, whole-cell patch-clamp recordings paired with retrograde labeling in adult
385 animals—albeit confounded by the absence of relevant synaptic inputs *in vivo*—is a
386 powerful technique that future studies should continue to use to aid in the investigation of
387 this population of neurons both in health and disease.

388 Our *ex vivo* results are consistent with electrophysiological recording in other DMV
389 populations. DMV neurons demonstrate an on-going activity phenotype [32,47,48]. This was

390 true in the present study as ~57% of $CVN^{DMV}$ demonstrated a spontaneously active firing
391 pattern during the recording period. With regards to CVNs, this on-going firing activity is
392 unique to $CVN^{DMV}$ since no $CVN^{NA}$ recorded exhibited any spontaneous activity in our
393 slice preparation, which is also consistent with previous results from $CVN^{NA}$ [31]. While
394 future studies will need to demonstrate how this spontaneous activity is generated, it is
395 consistent with the intrinsic pace-making properties of other DMV neurons. However, it
396 also suggests that $CVN^{DMV}$ may represent a functionally discrete circuit for cardiac-related
397 vagal motor output. Previous studies suggest that $CVN^{DMV}$ have little respiratory-related
398 burst activity, despite robust lung-related afferent activity [33], which is in contrast to the
399 $CVN^{NA}$ which show robust respiratory-related burst activity both *in vivo* and *ex vivo* [9].
400 While we are only beginning to elucidate the complexity of vagal circuits as it relates to
401 any vagal motor output, there is increasing evidence for distinct circuits related to vagal
402 sensory afferents. Similar distinct circuits also likely exist in vagal motor nuclei [41,49,50].
403 While some parallel circuits have converging anatomy and function, they may be distinct
404 in terms of their physiological roles [50]. Finally, $CVN^{DMV}$ demonstrated a significantly higher
405 input resistance, higher number of spiking activity to current injections, and smaller size
406 compared to $CVN^{NA}$. During optogenetic stimulation, $CVN^{DMV}$s were also silenced for
407 several seconds after stimulation implicating additional electrophysiological properties
408 (i.e., unique ion channel contributions or stimulation-induced plasticity in neurotransmitter
409 contributions) that could be investigated. Therefore, $CVN^{DMV}$ are more excitable than
410 $CVN^{NA}$. In other brain regions, this type of behavior confers a coincidence detection
411 phenotype over a simple integrator [51]. Therefore, future work should continue to

412 investigate how CVNs in NA and DMV differ in their microcircuit construction in relation to
413 the basic circuit building blocks of critical homeostatic regulating networks.

414 Despite historical controversy about the capacity of $CVN^{DMV}$ to impact HR, our
415 results demonstrate that optogenetic and chemogenetic activation of Chat+ DMV neurons
416 each caused robust bradycardia (~56% and ~65.5% of resting HR, respectively) in
417 awake, behaving mice. Cardioinhibitory responses using optogenetic techniques in
418 urethane-anesthetized rats and ketamine/xylazine-anesthetized mice demonstrated
419 variable strength of the response [18,21], implicating differences in anesthesia for differences
420 in effect size. Alternatively, previous species used (namely cats and rats) may exhibit a
421 lesser degree of DMV-activation driven bradycardia than mice because of differences in
422 vagal tonus. Since mice have a lower vagal tone than rats for example [52-54], $CVN^{DMV}$
423 activation in mice may recruit a larger number of $CVN^{DMV}$ which were not previously
424 active. Although it is possible that fast decay kinetics of $NpHR^{EYFP}$ in the Ai39 mouse line
425 limited the ability to significantly inhibit DMV neurons [36], the lack of an effect on HR of
426 optogenetic inhibition of DMV in mice is similar to previous reports using inhibitory
427 chemogenetic receptors [17]. Therefore, while the present study introduced a significant
428 refinement of techniques using $Chat^{cre}$ mice to eliminate the impact of known interneurons
429 within DMV, it may suggest that $CVN^{DMV}$ activity is not necessary for generation of resting
430 HR, similar to previous report [17].

431 While our Chat-targeted approach avoids influence of interneurons within DMV,
432 the anatomical proximity of vagal axons from NA and the optical fiber in DMV [14] raises
433 the possibility that DMV stimulation resulted in axonal stimulation of $CVN^{NA}$ neurons.
434 However, we failed to detect c-Fos expression in NA and DMV contralateral to the optical

435 fiber, despite robust c-Fos immunoreactivity in the ipsilateral DMV. In addition, direct
436 photostimulation of the vagus nerve in Chat$^{cre}$;ChR2 animals did not produce bradycardia.
437 Finally, the more specifically targeted chemogenetic receptor hM3Dq expressed in DMV,
438 but not other nearby cholinergic regions such as NA or hypoglossal neurons, caused a
439 similar cardioinhibition to DMV stimulation in Chat$^{cre}$;ChR2. Taken together, these data
440 provide robust evidence that solely activating DMV is sufficient for cardioinhibition (Figure
441 1D).

442 As expected, pharmacological testing confirmed that DMV stimulation-induced
443 bradycardia requires mACh receptor activation in mice, since scopolamine (but not
444 atenolol) and MA abolished optogenetically- and chemogenetically-induced bradycardia,
445 respectively. Notably, while the traditional concept of vagal motor signaling to cardiac
446 tissue requires nicotinic receptor-dependent communication between preganglionic and
447 postganglionic parasympathetic neurons, some studies report that intracardiac ganglia
448 harvested from SA node also show mACh receptor-dependent neurotransmitter and
449 calcium mobilization [55]. Additional studies have attributed pharmacological differences in
450 vagal fiber activation to C-fiber (presumably from DMV) versus B-fiber bradycardia
451 (presumably from NA) since hexamethonium did not block the HR responses to non-
452 myelinated fiber activation in these studies [56]. Still, it is important to note that the
453 aforementioned studies did not comment on whether postganglionic neurons were
454 isolated from cardiac nodal cells, nor did they directly address the effect of
455 neurotransmitter release on the observed HR responses. Our findings are in accordance
456 with the canonical signaling pathway between preganglionic and postganglionic

457 parasympathetic neurons, as pre-treatment with the mACh receptor antagonist,
458 scopolamine, completely abolished light-induced bradycardia in ChAT$^{cre}$;ChR2 mice.

459 Recent research suggests that HR can influence emotional states, supporting a
460 theory of emotion separately proposed by the physiologist Carl Lange and psychologist
461 William James over a century ago. As explained by James: "*My thesis […] is that the*
462 *bodily changes follow directly the Perception of the exciting fact, and that our feeling of*
463 *the same changes as they occur IS the emotion."* [57]. In other words, the James-Lange
464 theory holds that HR does not increase because of anxiety; rather, the perception of HR
465 increase is the anxiety. Consistent with this theory, a recent study in mice demonstrated
466 that optogenetically increasing HR is sufficient to drive anxiety-like behaviors in the
467 elevated plus maze [29]. Inversely, beta-blockers such as propranolol, which robustly
468 decrease HR [58], also reduce anxiety-like behaviors in mice [59,60]. Beta-blockers and other
469 drugs which decrease HR have shown promise for treating anxiety and related disorders
470 [61], though the mechanism is not yet known. Studies of brain activity in humans and mice
471 suggest the insular cortex may play a key role in sensing HR and other interoceptive cues
472 [29,62-64] and so could couple the perception of HR to emotional state.

473 Importantly, however, while our study is the first to our knowledge to demonstrate
474 a correlation between vagally-mediated bradycardia and anxiolysis, more research is
475 needed to establish a causal relationship. Our results with the cardioselective M2 receptor
476 antagonist AQ-RA 741 [45], which does not appear to cross the blood-brain barrier [46],
477 suggests a cardiogenic mechanism for the anxiolysis we observed when activating DMV
478 neurons. For instance, one possibility is that DMV decreases anxiety-like behavior by
479 decreasing HR. This would agree with recent studies showing that optogenetically

480 increasing HR is anxiogenic [29], whereas pharmacologically decreasing HR is anxiolytic
481 [65]. Indeed, the M2 receptors blocked by AQ-RA 741 are enriched in the heart relative to
482 other organs innervated by the DMV [45,66] and are necessary for vagally-mediated
483 bradycardia [67]. However, M2 receptors are also present in the gastrointestinal tract where
484 they interact with M3 receptors to modulate smooth muscle contraction [68]. Therefore, our
485 results do not rule out the possibility that DMV decreases anxiety-like behavior through
486 its projections to the gut [68,69]. Further research, e.g., targeting organ-specific DMV
487 circuits, is needed to establish the mechanism by which DMV neurons can decrease
488 anxiety. Whether other physiological functions of DMV, such as gut motility, glucose
489 metabolism, and suppressing inflammation [58], are involved remains unknown.

490 In summary, this study demonstrates the existence of $CVN^{DMV}$ neurons and their
491 ability to suppress HR and anxiety-like behavior. The cardioinhibitory and behavioral
492 effects both require mACh receptor activity, and our results also suggest that nACh
493 receptors are involved in the signaling between $CVN^{DMV}$ and cardiac parasympathetic
494 neurons, implicating canonical vagal pathways in DMV's facilitation of cardioinhibitory
495 activity. $CVN^{DMV}$ also has distinct electrophysiological properties, namely spontaneous
496 firing activity and higher $R_{input}$, compared to $CVN^{NA}$ *in slice*. Therefore, we further
497 speculate that $CVN^{DMV}$ represents a unique population of CVNs, distinct from the more
498 thoroughly characterized $CVN^{NA}$. Further research is needed to identify the molecular
499 profile of $CVN^{DMV}$, the mechanisms underlying their distinct electrophysiological
500 properties, and their physiological role.

501

**ACKNOWLEDGEMENTS:** Funding was provided by a Pathway to Stop Diabetes Initiator Award 1-18-INI-14, an NIH R01 HL153916 to J.N.C., an NIH R01HL157366 to C.R.B. and an NIH T32 HL007446 for M.M.S.

**AUTHOR CONTRIBUTIONS.** M.M.S., N.J.C., L.S.K., M.J., S.B.G.A., J.N.C., and C.R.B. designed experiments. M.M.S, L.E., and S.F. performed optogenetic and cardiac tracing studies, including HR analysis, and all histology/immunofluorescence. L.E. and C.R.B. performed electrophysiological studies. A question from G.E.H. inspired the study of anxiety-like behavior. N.J.C., L.S.K., M.E.C., and P.C.M. performed chemogenetic study of HR and anxiety-like behavior. N.J.C. and L.S.K. performed histology and immunofluorescence experiments related to chemogenetic studies. M.M.S., N.J.C., J.N.C., L.E., and C.R.B. prepared figures. M.M.S., N.J.C., L.S.K., C.R.B., and J.N.C. wrote the manuscript with input from all authors.

**DECLARATION OF INTEREST**

Authors declare no competing interest.

**FIGURE CAPTIONS:**

**Figure 1:** Optogenetic stimulation of DMV elicits bradycardia in male and female mice. Genetic crossbreeding paradigm used to generate transgenic mice harboring loxP-flanked ChR2 in Chat-positive motor neurons (A). Photostimulation-evoked action potentials from DMV motor neurons pace to 20 Hz stimulation (B). Representative diagram illustrating confirmed locations of optogenetic probes (C). Representative

525 images of DMV (top) and NA (bottom) stained for the neuronal activation marker, c-Fos
526 (middle panel; red) and GFP (left panel; green) immunoreactivity confirming c-Fos
527 activation in DMV, but not NA, after DMV photostimulation (D). Schematic illustrating time
528 course of optogenetic studies in awake mice (E). Representative trace (F) and mean HR
529 (G) showing optogenetic stimulation of DMV produced a bradycardia in mice expressing
530 $Chat^{cre}$;ChR2 but not in $Chat^{cre}$ mice. Representative trace (H) and mean HR (I) showing
531 *i.p.* muscarinic parasympathetic blocker, methyl-scopolamine, eliminated the
532 photostimulation-induced bradycardia, while sympathetic blockage with β-1 receptor
533 blocker atenolol mildly reduced this bradycardia. Representative images of probe site
534 (top) and immunohistochemical staining of NA showing c-Fos activation after stimulation
535 of NA (J). Representative trace (K) and mean HR (L) showing the nicotinic antagonist,
536 hexamethonium *(i.p.)* abolished photostimulation-induced bradycardia in both DMV and
537 NA. Bars represent mean and SEM. Blue bars/shading indicates light stimulation. *$p \leq$
538 $0.05$, **$p \leq 0.01$, ***$p \leq 0.001$, ****$p \leq 0.0001$.
539
540 **Figure 2:** DMV innervates cardiac tissue through the vagus nerve in male mice.
541 Schematic showing injection into the epicardial fat pad and labeling in both CVN brain
542 regions (A). Representative images of DMV and NA after cardiac injection of retrograde
543 tracers, rhodamine (left in red) and cholera toxin subunit B (CT-B; right in green) (B). Both
544 rhodamine and CT-B significantly labeled cardiac projecting neurons in NA and DMV (C).
545 Representative images of DMV after a right cervical vagotomy (C). Representative image
546 (D) and mean cell count (E) showing a right cervical vagotomy significantly attenuated

547 $CVN^{DMV}$ numbers ipsilateral to vagotomy. Bars represent mean and SEM. *p ≤ 0.05, **p
548 ≤ 0.01, ***p ≤ 0.001, ****p ≤ 0.0001.
549
550 **Figure 3:** Differential electrophysiological properties of $CVN^{DMV}$ compared to $CVN^{NA}$ in
551 male mice. Rhodamine-positive DMV neurons showing pipette (top) and rhodamine
552 (bottom; red) (A). Representative immunofluorescence image of $CVN^{DMV}$ showing
553 biocytin recovered patched cardiac-labeled neurons are cholinergic (B). Representative
554 trace (C) and mean firing rate (D) of $CVN^{DMV}$ neurons show significantly higher
555 spontaneous firing rates compared to $CVN^{NA}$, with the majority of $CVN^{DMV}$ firing. No
556 statistical differences in resting membrane potential were found between $CVN^{DMV}$ and
557 $CVN^{NA}$ (E). Representative traces of membrane responses from $CVN^{NA}$ (top) and $CVN^{DMV}$
558 (bottom) to stepped current injections (F). Current-voltage (I-V) relationship graph
559 obtained from $CVN^{NA}$ and $CVN^{DMV}$ (G). $R_{input}$ was higher in $CVN^{DMV}$ compared to $CVN^{NA}$
560 (H). Representative action potential responses in $CVN^{NA}$ (top) and $CVN^{DMV}$ (bottom) in
561 response to 300 pA injection of direct depolarizing current (I). Action potential response
562 curves were higher in $CVN^{DMV}$ compared to $CVN^{NA}$ in response to 50 pA-step injections
563 of direct depolarizing current (J). *p ≤ 0.05, **p ≤ 0.01, ***p ≤ 0.001, ****p ≤ 0.0001.
564
565 **Figure 4:** Chemogenetic stimulation of DMV produces bradycardia and reduces anxiety
566 in both male and female mice. Illustration of coronal hindbrain section showing injection
567 site and *Chat* and *Phox2b* expression (A, top left); Schematic of AAV1-CreON/FlpON-
568 hM3Dq-HA viral construct (A, bottom); Venn diagram showing expected expression of
569 hM3Dq-HA and H2b-GFP (A, top right). Representative images of rostral, intermediate,

570 caudal DMV and NA stained for HA (magenta) and H2b-GFP (green) immunoreactivity in
571 Chat$^{Cre}$;Phox2b$^{Flp}$;R26$^{ds\text{-}HTB}$ mice after DMV injection of AAV1-CreON/FlpON-hM3Dq-HA
572 (B). Percentage of H2b-GFP+ cells immunoreactive for hM3Dq-HA in the rostral,
573 intermediate and caudal DMV and NA (C). Effect of CNO on HR in DMV-hM3Dq mice
574 over 24-hour period. CNO (1mg/kg, *i.p.)* injected at time = 0 min (D). Effect of *i.p.* saline,
575 CNO and CNO+MA on HR in DMV-hM3Dq (magenta) and control mice (black);
576 comparisons are to baseline (E). Schematic of open field experiment (F). Effects of *i.p.*
577 saline vehicle and CNO on time in the center of the open field, in seconds (G). Correlation
578 between changes in HR and center time between saline and CNO conditions in DMV-
579 hM3Dq mice (H).Schematic of elevated plus maze (EPM) experiment (I). Effects of *i.p.*
580 saline vehicle, CNO and CNO+MA administration on time spent moving in the elevated
581 plus maze, in seconds (J). Effect of *i.p.* saline vehicle, CNO and CNO+MA administration
582 on open-arm time in the elevated plus maze, in seconds (K). Effect of *i.p.* saline vehicle,
583 CNO and CNO+AQ administration on open-arm time in the elevated plus maze, in
584 seconds. (L). Correlation between changes in HR and open-arm time between saline and
585 CNO conditions in DMV-hM3Dq mice (M). Effects of *i.p.* MA and AQ-RA-741 on open-
586 arm time in elevated plus maze, compared to saline; same saline, CNO, and CNO+MA
587 data as in Figure 4K (N). *$p \leq 0.05$, **$p \leq 0.01$, ***$p \leq 0.001$, ****$p \leq 0.0001$.
588
589 **Supplemental Figure 1:** Representative images of intermediate DMV hemisphere
590 stained for H2b-GFP (green) and fluorogold immunoreactivity (blue) in
591 Chat$^{Cre}$;Phox2b$^{Flp}$;R26$^{ds\text{-}HTB}$ mice after *(i.p.)* systemic injection of retrograde tracer
592 Flurogold (136 of 139, 97.8%, Fluorogold+ DMV neurons were also H2b-GFP+); n=4

593 mice) (A). Representative images of intermediate DMV stained for HA (magenta) and
594 H2b-GFP (green) immunoreactivity in R26$^{ds\text{-}HTB}$ mice (Cre-/Flp-) after DMV injection of
595 AAV1-CreON/FlpON-hM3Dq-HA (B). Effect of *i.p.* saline (white), CNO (magenta) and
596 CNO+MA (green) on HR in DMV-hM3Dq and control mice; relative to vehicle (C). Effect
597 of saline or CNO on control mice, which lack hM3Dq expression, open-arm time in the
598 elevated plus maze, n=8 mice (D). Effect of saline, CNO and CNO+MA in DMV-hM3Dq
599 mice on head dip events and velocity in the elevated plus maze (E-F). Effect of saline,
600 CNO and CNO+AQ on HR in DMV-hM3Dq (magenta) mice; same experimental design
601 and baseline, saline, and CNO data as in Figure 4E (G). *$p \leq 0.05$, **$p \leq 0.01$, ***$p \leq$
602 $0.001$, ****$p \leq 0.0001$.

603 **LEAD CONTACT**

604 Further information and requests for resources and reagents should be directed to
605 and will be fulfilled by the lead contact, Carie R. Boychuk (BoychukC@missouri.edu).

606 **MATERIALS AVAILABILITY**

607 All data reported in this paper will be shared by the lead contact upon request. This
608 study did not generate new unique reagents or report original code.

609

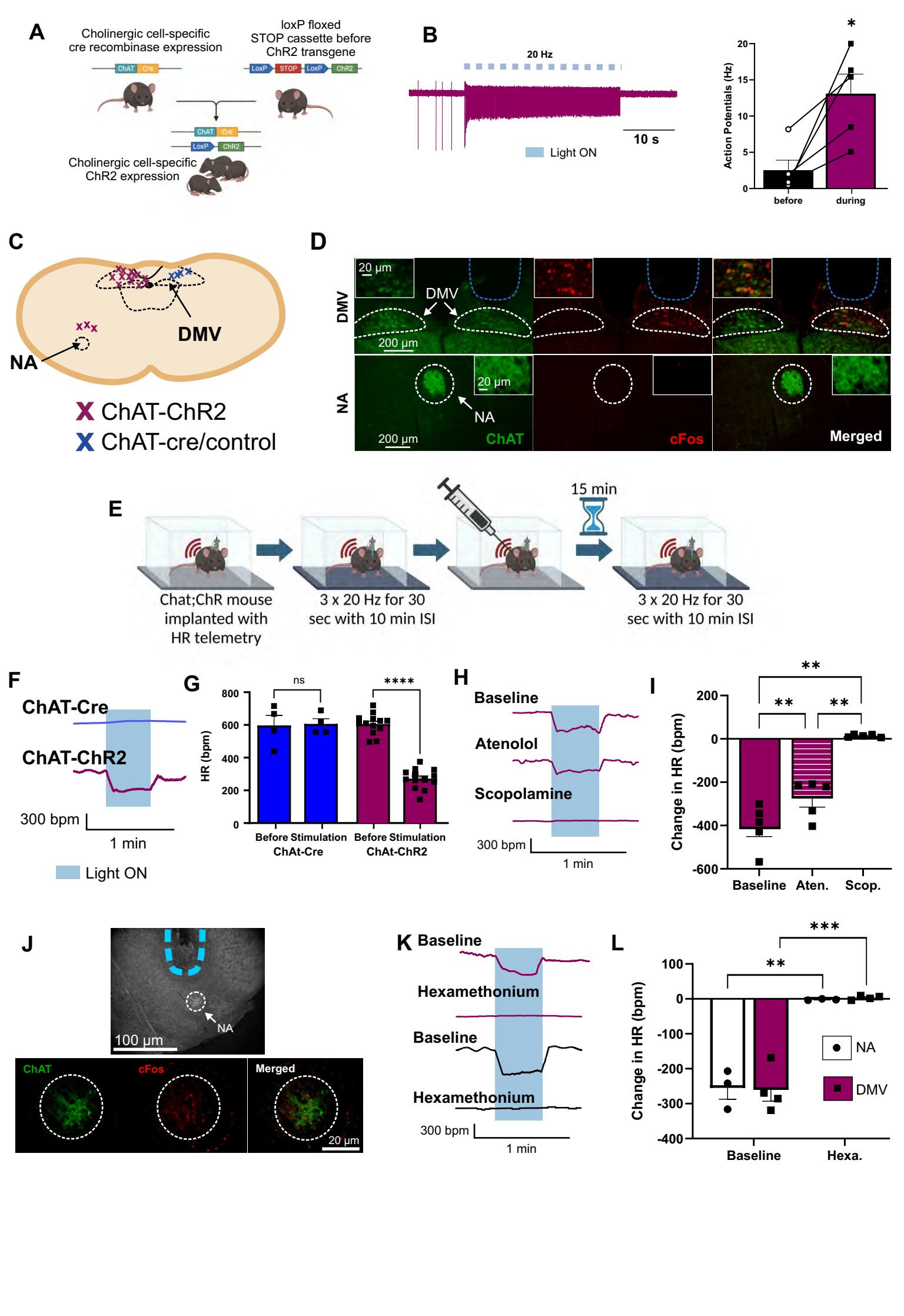
A
Cholinergic cell-specific cre recombinase expression
loxP floxed STOP cassette before ChR2 transgene
ChAT
Cre
LoxP
STOP
ChR2
Cholinergic cell-specific ChR2 expression
B
20 Hz
10 s
Light ON
Action Potentials (Hz)
before
during
C
DMV
NA
ChAT-ChR2
ChAT-cre/control
D
20 µm
DMV
200 µm
NA
ChAT
cFos
Merged
E
15 min
Chat;ChR mouse implanted with HR telemetry
3 x 20 Hz for 30 sec with 10 min ISI
3 x 20 Hz for 30 sec with 10 min ISI
F
ChAT-Cre
ChAT-ChR2
300 bpm
1 min
Light ON
G
ns
****
HR (bpm)
Before Stimulation ChAt-Cre
Before Stimulation ChAt-ChR2
H
Baseline
Atenolol
Scopolamine
300 bpm
1 min
I
Change in HR (bpm)
Baseline
Aten.
Scop.
J
NA
100 µm
ChAT
cFos
Merged
20 µm
K
Baseline
Hexamethonium
Baseline
Hexamethonium
300 bpm
1 min
L
Change in HR (bpm)
NA
DMV
Baseline
Hexa.

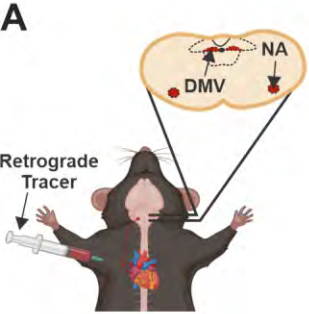
A
NA
DMV
Retrograde
Tracer

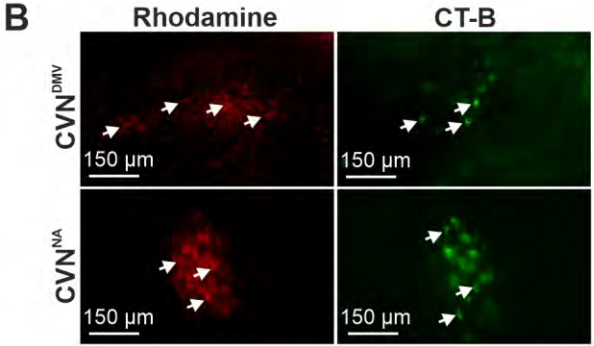
B
Rhodamine
CT-B
CVN^DMV
CVN^NA
150 µm
150 µm
150 µm
150 µm

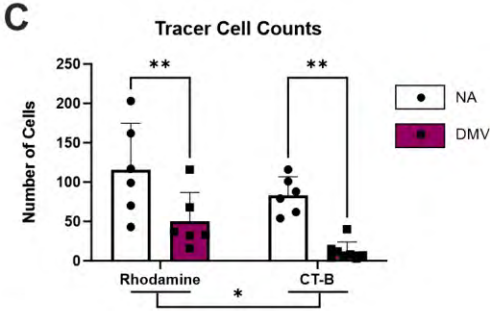
C
Tracer Cell Counts
Number of Cells
250
200
150
100
50
0
**
**
*
Rhodamine
CT-B
NA
DMV

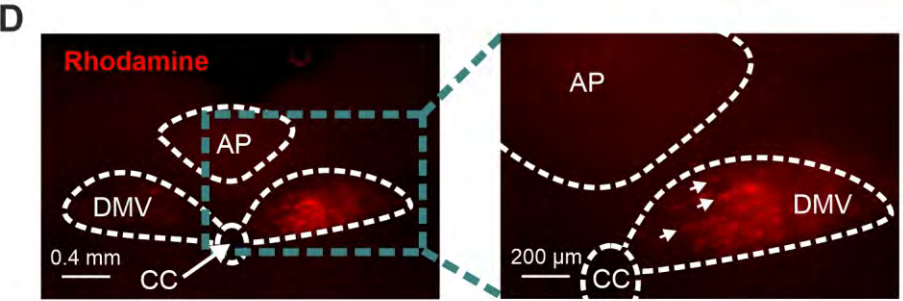
D
Rhodamine
AP
DMV
CC
0.4 mm
AP
DMV
CC
200 µm

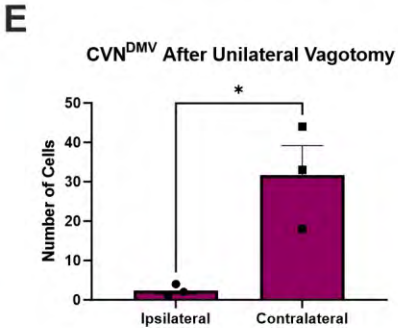
E
CVN^DMV After Unilateral Vagotomy
Number of Cells
50
40
30
20
10
0
*
Ipsilateral
Contralateral

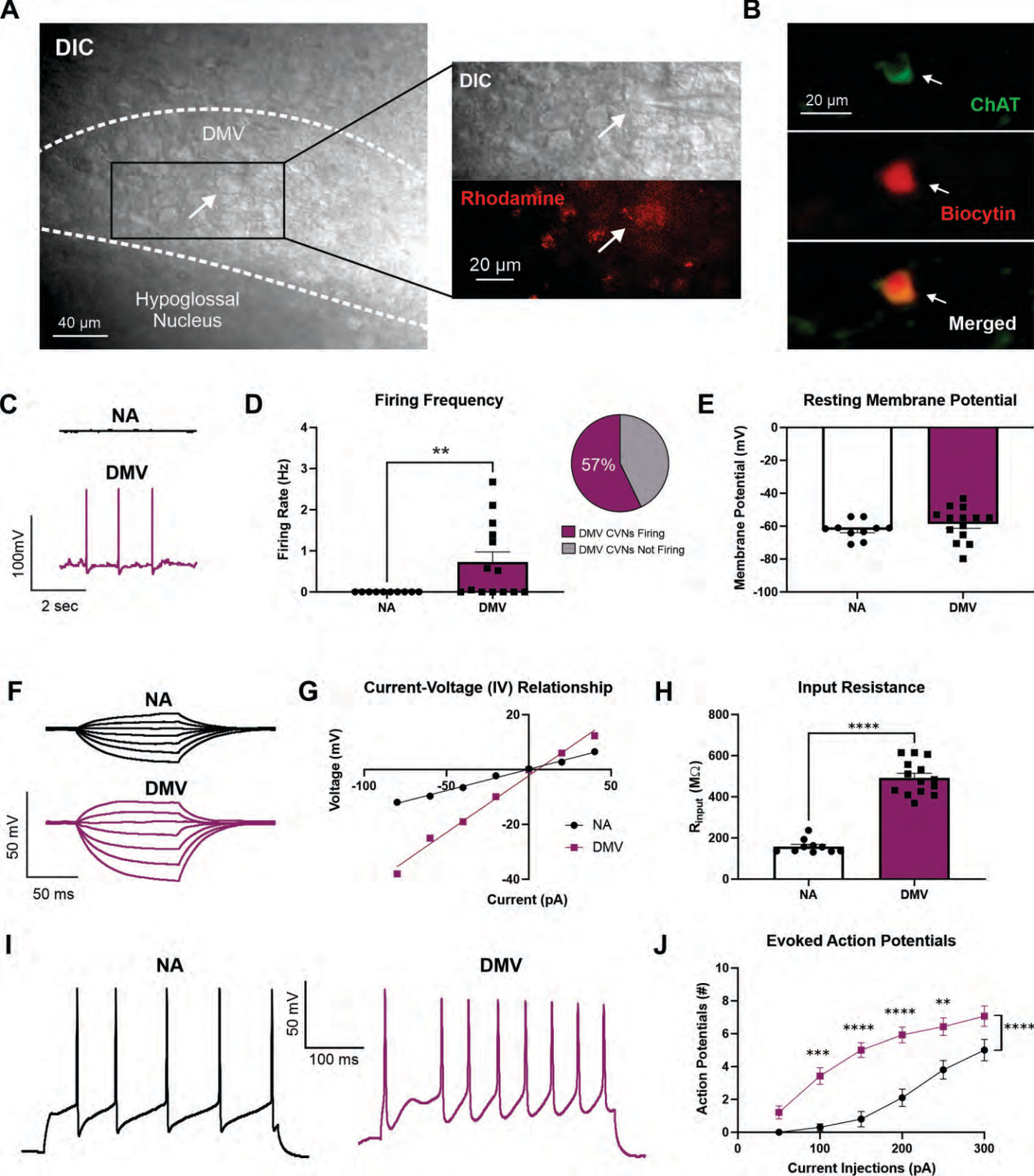
A
DIC
DMV
Hypoglossal Nucleus
40 µm
DIC
Rhodamine
20 µm
B
20 µm
ChAT
Biocytin
Merged
C
NA
DMV
100mV
2 sec
D
Firing Frequency
Firing Rate (Hz)
**
NA
DMV
57%
DMV CVNs Firing
DMV CVNs Not Firing
E
Resting Membrane Potential
Membrane Potential (mV)
NA
DMV
F
NA
DMV
50 mV
50 ms
G
Current-Voltage (IV) Relationship
Voltage (mV)
Current (pA)
NA
DMV
H
Input Resistance
$R_{input}$ (MΩ)
****
NA
DMV
I
NA
DMV
50 mV
100 ms
J
Evoked Action Potentials
Action Potentials (#)
Current Injections (pA)
***
****
****
**
****

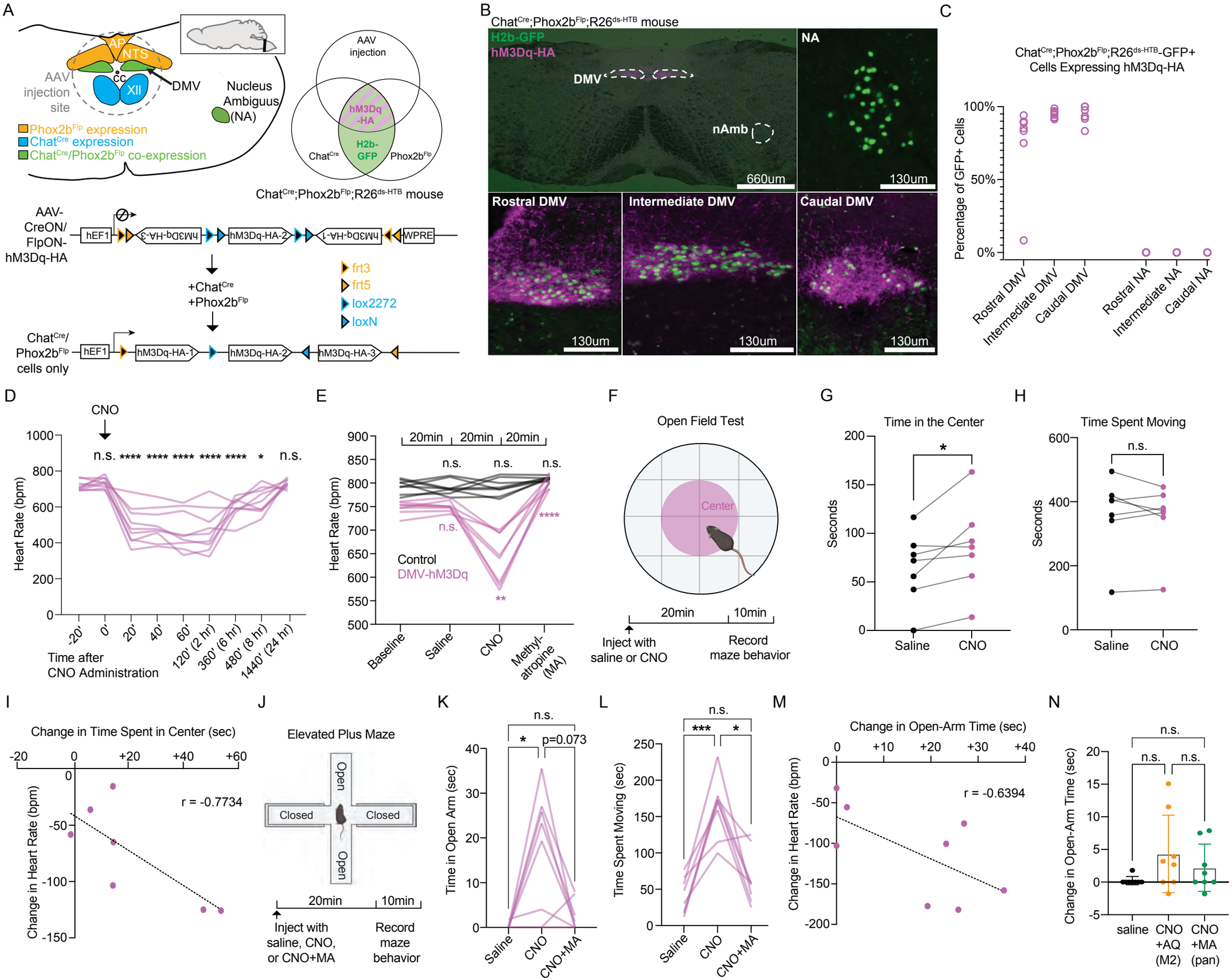
A
AP
NTS
AAV injection site
cc
XII
DMV
Nucleus Ambiguus (NA)
Phox2b^Flp expression
Chat^Cre expression
Chat^Cre/Phox2b^Flp co-expression
AAV injection
hM3Dq -HA
H2b-GFP
Chat^Cre
Phox2b^Flp
Chat^Cre;Phox2b^Flp;R26^ds-HTB mouse
AAV-CreON/FlpON-hM3Dq-HA
hEF1
hM3Dq-HA-3
hM3Dq-HA-2
hM3Dq-HA-1
WPRE
+Chat^Cre
+Phox2b^Flp
frt3
frt5
lox2272
loxN
Chat^Cre/Phox2b^Flp cells only
hM3Dq-HA-1
hM3Dq-HA-2
hM3Dq-HA-3
B
Chat^Cre;Phox2b^Flp;R26^ds-HTB mouse
H2b-GFP
hM3Dq-HA
DMV
nAmb
660um
NA
130um
Rostral DMV
Intermediate DMV
Caudal DMV
130um
130um
130um
C
Chat^Cre;Phox2b^Flp;R26^ds-HTB-GFP+ Cells Expressing hM3Dq-HA
Percentage of GFP+ Cells
100%
50%
0%
Rostral DMV
Intermediate DMV
Caudal DMV
Rostral NA
Intermediate NA
Caudal NA
D
CNO
n.s. **** **** **** **** **** * n.s.
Heart Rate (bpm)
1000
800
600
400
200
0
-20'
0'
20'
40'
60'
120' (2 hr)
360' (6 hr)
480' (8 hr)
1440' (24 hr)
Time after CNO Administration
E
20min
20min
20min
n.s.
n.s.
n.s.
****
n.s.
Control
DMV-hM3Dq
**
Heart Rate (bpm)
900
850
800
750
700
650
600
550
500
Baseline
Saline
CNO
Methyl-atropine (MA)
F
Open Field Test
Center
20min
10min
Inject with saline or CNO
Record maze behavior
G
Time in the Center
*
Seconds
200
150
100
50
0
Saline
CNO
H
Time Spent Moving
n.s.
Seconds
600
400
200
0
Saline
CNO
I
Change in Time Spent in Center (sec)
-20
0
+20
+40
+60
r = -0.7734
Change in Heart Rate (bpm)
0
-50
-100
-150
J
Elevated Plus Maze
Open
Closed
Closed
Open
20min
10min
Inject with saline, CNO, or CNO+MA
Record maze behavior
K
n.s.
*
p=0.073
Time in Open Arm (sec)
40
30
20
10
0
Saline
CNO
CNO+MA
L
n.s.
***
*
Time Spent Moving (sec)
250
200
150
100
50
0
Saline
CNO
CNO+MA
M
Change in Open-Arm Time (sec)
0
+10
+20
+30
+40
r = -0.6394
Change in Heart Rate (bpm)
0
-50
-100
-150
-200
N
n.s.
n.s.
n.s.
Change in Open-Arm Time (sec)
20
15
10
5
0
-5
saline
CNO +AQ (M2)
CNO +MA (pan)

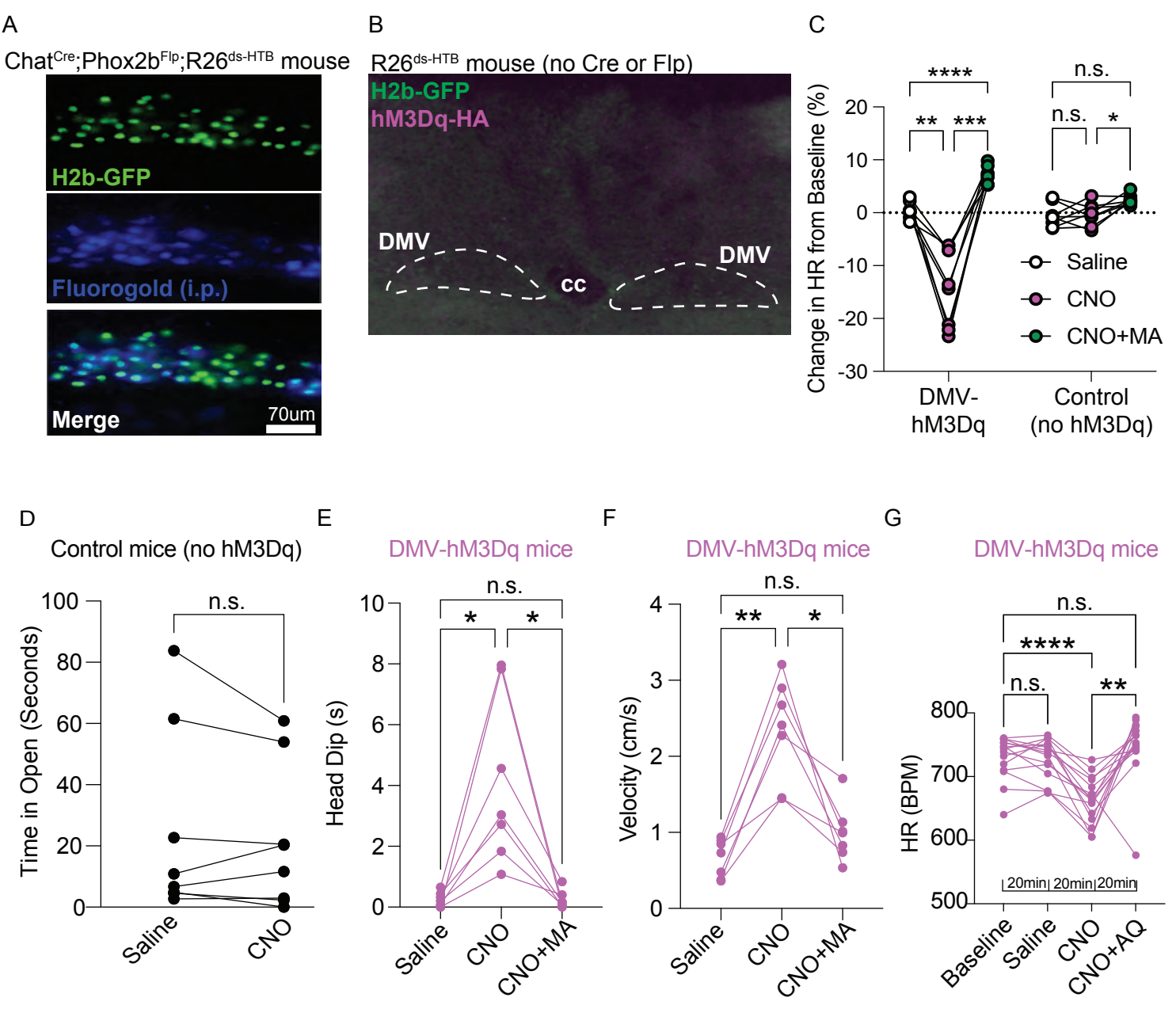
A
Chat$^{Cre}$;Phox2b$^{Flp}$;R26$^{ds\text{-}HTB}$ mouse
H2b-GFP
Fluorogold (i.p.)
Merge
70um
B
R26$^{ds\text{-}HTB}$ mouse (no Cre or Flp)
H2b-GFP
hM3Dq-HA
DMV
cc
DMV
C
Change in HR from Baseline (%)
20
10
0
-10
-20
-30
****
**
***
n.s.
n.s.
*
Saline
CNO
CNO+MA
DMV-hM3Dq
Control (no hM3Dq)
D
Control mice (no hM3Dq)
Time in Open (Seconds)
100
80
60
40
20
0
n.s.
Saline
CNO
E
DMV-hM3Dq mice
Head Dip (s)
10
8
6
4
2
0
n.s.
*
*
Saline
CNO
CNO+MA
F
DMV-hM3Dq mice
Velocity (cm/s)
4
3
2
1
0
n.s.
**
*
Saline
CNO
CNO+MA
G
DMV-hM3Dq mice
HR (BPM)
800
700
600
500
n.s.
****
n.s.
**
20min
20min
20min
Baseline
Saline
CNO
CNO+AQ